Spatiotemporal Changes and Driving Factors of Ecosystem Health in the Qinling-Daba Mountains

Xiang, Ting; Meng, Xiaoliang; Wang, Xinshuang; Xiong, Jing; Xu, Zelin

DOI
10.3390/ijgi11120600

Publication date
2022

Document Version
Final published version

Published in
ISPRS International Journal of Geo-Information

International Journal of
Geo-Information

Article

Spatiotemporal Changes and Driving Factors of Ecosystem Health in the Qinling-Daba Mountains

Ting Xiang [1], Xiaoliang Meng [1,*], Xinshuang Wang [2], Jing Xiong [3] and Zelin Xu [4]

1 School of Remote Sensing and Information Engineering, Wuhan University, Wuhan 430079, China
2 Shaanxi Geomatics Center, Ministry of Natural Resources, Xi'an 710054, China
3 Hubei Environmental Monitoring Central Station, Wuhan 430072, China
4 Department of Geoscience & Remote Sensing, Delft University of Technology, P.O. Box 5048, 2600 Delft, The Netherlands
* Correspondence: xmeng@whu.edu.cn

Abstract: Rapid industrialization and urbanization have accelerated land-use changes in mountainous areas, with dramatic impacts on ecosystem health. In particular, the Qinling-Daba Mountains, as China's central water tower, ecological green lung, and biological gene bank, have rich resource endowments and extremely high ecological value and are an important protective wall to China's ecological security. Therefore, understanding the level of ecosystem health and its drivers in the research area contributes to the conservation and restoration of the mountain ecosystem. Based on remote sensing image data and land-use data from 2000 to 2020, we explored the spatial characteristics of ecosystem health, and supplemented with socio-economic data to explore its driving factors. The results show that (1) the ecosystem health in the study area has been continuously improved during the study period, and the regional differences in ecological organization are the most prominent; (2) the level of ecosystem health in the Qinling-Daba Mountains has been spatially improved from the peripheral areas to the central area, showing significant spatial autocorrelation and local spatial aggregation; (3) the ecosystem health is influenced by a combination of natural and anthropogenic factors, among which the negative effect of GRDP is mainly concentrated in the eastern region, the negative effect of the proportion of built-up land gradually spreads to the western region, and the positive effect of the proportion of forest land has a large scale. This study contributes to a better understanding of ecosystem health in mountainous counties in China and provides useful information for policymakers to formulate ecological and environmental management policies.

Keywords: ecosystem health; spatiotemporal characteristics; driving factors; GWR; Qinling-Daba Mountains

check for updates

Citation: Xiang, T.; Meng, X.; Wang, X.; Xiong, J.; Xu, Z. Spatiotemporal Changes and Driving Factors of Ecosystem Health in the Qinling-Daba Mountains. *ISPRS Int. J. Geo-Inf.* **2022**, *11*, 600. https://doi.org/10.3390/ijgi11120600

Academic Editors: Wolfgang Kainz, Maurizio Pollino and Giuseppe Modica

Received: 9 October 2022
Accepted: 24 November 2022
Published: 29 November 2022

1. Introduction

China's massive and rapid urbanization has accelerated national economic growth at great costs of resource use and environmental pollution, causing many ecological consequences, such as farmland occupation [1], landscape fragmentation [2], energy shortages [3], air pollution [4], and reduced biodiversity [5], which have threatened the sustainable development of the whole country. Ecosystems are facing unprecedented shocks, and ecosystem health issues [6] have become a serious challenge to achieve green and sustainable development. Therefore, it is necessary to conduct a systematic assessment of ecosystem health to provide a scientific basis for managers to formulate policies.

A healthy ecosystem provides the material foundation and ecological services for human survival [7], and it also plays a critical role in maintaining and improving urban ecosystem function [8]. Ecosystems are large and complex, and a systematic assessment of ecosystem health requires a comprehensive consideration of multiple aspects. Based on the statistics of physical, ecological, and socioeconomic, pressure–state–response [9–11], driver–pressure–state–impact [12], driver–pressure–state–impact–response [13], and other methods to construct a system of indicators, and the analytic hierarchy process is often used to give weight to the indicators. These models are not good measures of land-use/land-cover (LULC) changes and shifts in landscape patterns, which not only affect the provision of essential ecosystem services for human health and well-being but can also misestimate the self-mitigation capacity of ecosystems. The vigor–organization–resilience (VOR) model is widely accepted for its simplicity of calculation and focus on LULC changes. Ecosystem vigor, ecosystem organization, and ecosystem resilience evaluate the health level of ecosystems in a comprehensive manner in terms of ecosystem primary productivity, structural stability, and recovery ability, respectively [14–16]. In a comprehensive measure of the natural condition of the ecosystem, we used the VOR model to quantitatively evaluate the level of ecosystem health in the Qinling-Daba Mountains.

Exploring the factors influencing ecosystem health is also a pressing issue. Methods such as correlation analysis, principal component analysis, regression analysis, and geographical detectors have been applied to discuss the relationship between ecosystem health and its drivers, especially the impact of human activities on ecosystem health at the regional scale [17–20]. However, traditional statistical and spatial analysis methods do not reflect the spatiotemporal variability of different drivers of geographic processes, which may limit practical decision-making for ecological environment management policies [21]. Compared with traditional statistical analysis methods, geographically weighted regression (GWR) models can not only analyze the relative importance of drivers but also graphically represent the spatial pattern generated under parameter estimation and represent the spatial pattern of the intensity of each driver's influence in the form of a map [22,23].

The Qinling-Daba Mountains are key areas for biodiversity protection and maintenance of ecological function [24]. With an ecological red line area of nearly 70%, the high forest cover provides a high-quality habitat for biodiversity [25]. As the north–south boundary of China, it has a unique geographical location and ancient geological history [26]. Studies of vegetation dynamics [27,28], forest structure [29], climate [30,31], and ecosystem services [32] in the region found an increase in vegetation coverage and significant spatial variation in ecosystem services in the Qinling-Daba Mountains. However, there is a lack of understanding of the study area ecosystems at the macro level, and few studies have analyzed ecosystem health and influencing factors in the region.

This paper analyzes the ecosystem health and its influencing factors in 120 counties in the Qinling-Daba Mountains from 2000 to 2020 using 30 m resolution remote sensing imagery and LULC data. This study aims to explore the following: (1) spatial characteristics of ecosystem health, mainly spatial correlation and spatial heterogeneity: (2) analysis of the factors influencing ecosystem health at the county scale. Our study will help managers to develop ecological conservation policies.

2. Materials and Methods

2.1. Study Area

The Qinling-Daba Mountains are in the central part of China, spanning 308,093 km^2, crossing Gansu, Shaanxi, Henan, Sichuan, Hubei, and Chongqing Municipality. It runs across five provinces and one municipality, including 120 counties (Figure 1). The topography of the Qinling-Daba Mountains is characterized by mountains and hills, gradually rising from east to west, and the altitude is very different. The southern part of the study area has a subtropical humid climate with an annual precipitation of 820 mm and an annual average temperature of 14 °C, while the northern part belongs to a warm temperate semi-humid climate with an annual precipitation of 520 mm and an annual average temperature of 10 °C [33]. The vegetation types are diverse and the zoning characteristics are obvious. It is a transition from warm-temperate deciduous broadleaf forests in the north to subtropical mixed broadleaf evergreen and deciduous forests in the south, with both northern and southern Chinese plant species. The study area is an interactive zone between China's humans, geography, climate, and biology, and it is also a fragile area of the ecological environment.

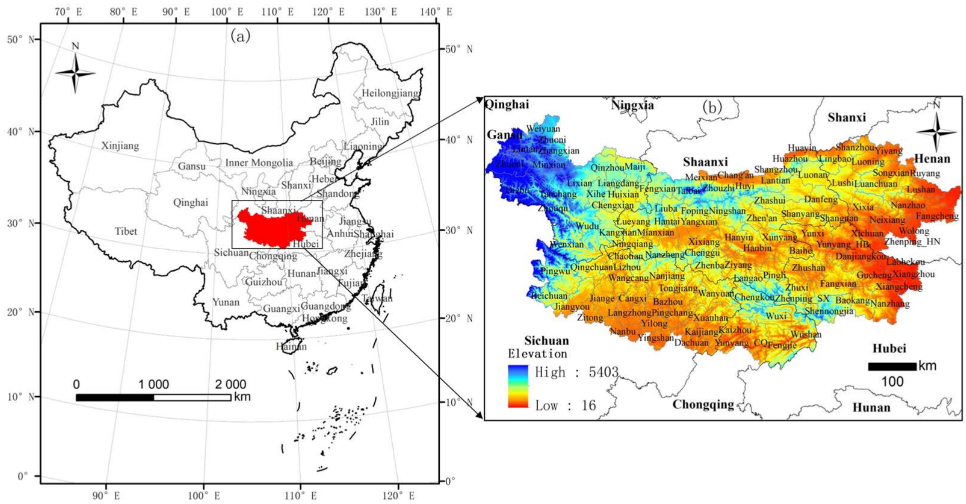

Figure 1. Geographical location map of the Qinling-Daba Mountains. (**a**) The location of the Qinling-Daba Mountains in China (**b**) The location and elevation of 120 counties and the corresponding six provinces.

2.2. Data Source and Preprocessing

Given the advantages of Google Earth Engine (GEE), such as free, easy data access and fast and batch processing of a huge number of images, this study obtained the normalized difference vegetation index (NDVI) through the rapid calculation of GEE. The data were obtained from the Landsat dataset provided by the Google Earth Engine (GEE) platform with a spatial resolution of 30 m. Image pre-processing needs to use GEE platform coding to search all the images in the study area in 2000, 2010 and 2020, and then project the data to the "WGS 84/UTM zone 48 N" coordinate system and normalize the data. Finally, the annual data are obtained by using the maximum synthesis method. The LULC data were derived from GlobeLand30 (http://www.globallandcover.com accessed on 9 May 2021), with a spatial resolution of 30 m. In this study, we merged woodlands and shrublands into forests and divided the land-use types in the Qinling-Daba Mountains into eight categories: farmland, forest, grassland, wetland, water body, impervious surface, glacier and snow, and bare land. Digital elevation model (DEM) data with 30 m spatial resolution come from ASTER GDEM (https://yceo.yale.edu/aster-gdem-global-elevation-data accessed on 15 May 2021).

The statistics of gross regional domestic product (GRDP) and population size (POP) of the research area for 2000, 2010, and 2020 are acquired from "Shaanxi Statistical Yearbook (2000–2021)", "Gansu Statistical Yearbook (2000–2021)", "Sichuan Statistical Yearbook (2000–2021)", "Henan Statistical Yearbook (2000–2021)", "Chongqing Mongolia Statistical Yearbook (2000–2021)", "Hubei Statistical Yearbook (2000–2021)" (National Bureau of Statistics, 2000–2021), the official websites of local governments, and other statistical outlets, with the county as a basic statistical unit. The proportion of built-up land (PBL) and the proportion of forest land (PFL) are calculated from LULC. Given the differences in the dimensions and magnitudes of the selected indicators, the data needed to be standardized before analysis using the following equations:

For positive indicators:

$$X_{ij} = \frac{x_{ij} - \min(x_j)}{max(x_j) - \min(x_j)} \tag{1}$$

For negative indicators:

$$X_{ij} = \frac{max(x_j) - x_{ij}}{max(x_j) - \min(x_j)} \tag{2}$$

where X_{ij} is the normalized value of indicator j in year i, x_{ij} represents the value of indicator j in year i; $max(x_j)$ and $\min(x_j)$, respectively, denote the maximum and minimum value of indicator j in all years. All the index values are in the range of [0, 1].

2.3. Methodology

This study assessed the ecosystem health level of the Qinling-Daba Mountains at the county scale. The vigor–organization–resilience model and Moran's I index were used to comprehensively evaluate the ecosystem health level and its spatial pattern of the study area, and the GWR model was used to analyze the impact of different factors on the ecosystem health. The specific research process is shown in Figure 2.

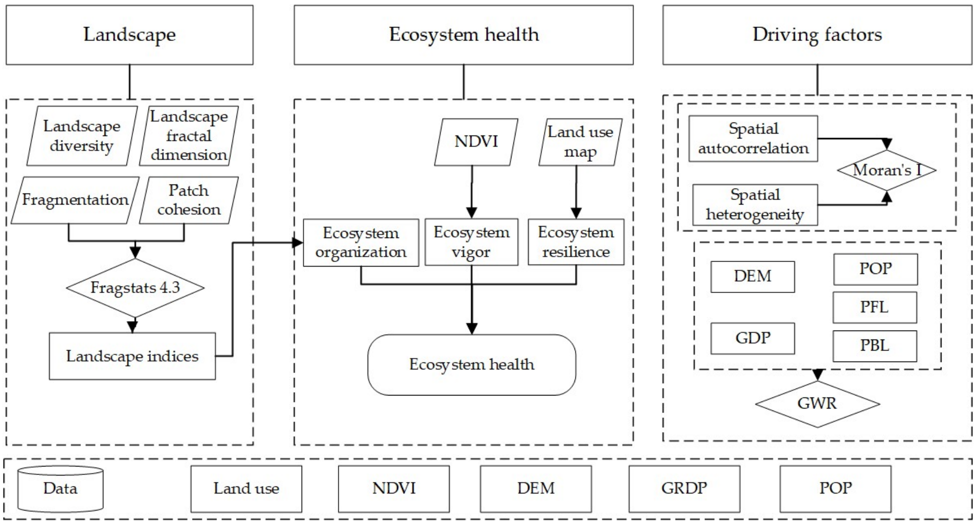

Figure 2. Overall framework of the research.

2.3.1. Vigor–Organization–Resilience Model

Ecosystem health depends on three traditional indicators: ecosystem vigor, organization, and resilience [34]. The ecosystem health index is assessed based on the VOR model. Ecosystem vigor refers to the metabolic capacity or primary productivity of the ecosystem. NDVI is widely proven to be an effective indicator for evaluating vegetation primary productivity [35,36]. NDVI is calculated using Landsat satellite images of a different time and multispectral bands [37–39].

Ecosystem organization (O) refers to the structural stability of an ecosystem and is related to spatial patterns. The landscape pattern index reflects landscape heterogeneity and landscape connectivity to measure spatial patterns. Landscape heterogeneity mainly studies spatial heterogeneity, measured by landscape diversity and landscape fractal dimension, corresponding to Shannon's diversity index and area-weighted mean patch fractal dimension index in this paper, respectively. Connectivity was measured by fragmentation and patch cohesion. Landscape connectivity is quantified by the landscape fragmentation index and landscape contagion index. As the dominant land-use type in mountainous areas, forest connectivity is determined by the fragmentation index and patch cohesion index of forest. It is calculated as follows:

$$O = 0.25 \times SHDI + 0.1 \times AMFRAC + 0.25 \times FN_1 + 0.1 \times CONTAG + 0.2 \times FN_2 + 0.1 \times COHESION \quad (3)$$

where O represents the ecosystem organization of spatial entities, SHDI is Shannon's diversity index, AMFRAC is area-weighted mean patch fractal dimension index, FN1 is the index of landscape fragmentation, CONTAG is the landscape contagion index, FN2 is the landscape fragmentation index of forest land, and COHESION is the index of the patch cohesion of forest land. These landscape indexes were obtained by Fragstats 4.2.

The ecosystem elasticity coefficient score (EC) of each LULC type in the Qinling-Daba Mountains developed as a weighted combination of resilience and resistance, given as [40]:

$$EC = 0.7 \times resil + 0.3 \times resist \tag{4}$$

In Table 1, The ecosystem elasticity coefficient (EC) of each land-use type in the study area is equal to 30% of the resilience coefficient (*resil*) plus 70% of the resistance coefficient (*resist*). The coefficients of resilience and resistance are determined according to the relevant papers [15,16] and the actual situation of the research area. Coefficients are assigned for the eight land-use types, with coefficients ranging from 0 to 1. Resilience refers to the ability of the ecosystem to return to its original state after being damaged by external disturbance factors, while resistance refers to the ability of an ecosystem to resist external disturbances and keep its own structure and function intact. Resistance and resilience are related, and typically, ecosystems with high resistance have low resilience. Compared with artificial ecosystems, natural ecosystems have stronger resistance and recovery ability. The resistance and resilience of human-dominated ecosystems are weak, and it is difficult to resist external disturbances and restore them to an original state, so the resilience and resistance coefficients of impervious surfaces and farmland are small. Water bodies and wetland ecosystems are more self-regulating and have a higher resistance and resilience capacity with larger coefficients. Bare land ecosystems are simple, and it is difficult to resist external disturbances, but they are easy to recover. Forests with complex species, strong biological chains, and tight ecosystems are resilient to external disturbances, while restoration to complex ecosystem structure and function takes more time. The ecosystem resilience (R) is defined as follows:

$$R = \sum_{k=1}^{m} P_k \times EC_k \tag{5}$$

where R is the ecosystem resilience of spatial entities, P_k is the proportion of the area of the land-use type k, EC_k is the ecosystem elasticity coefficient of land-use type k, and m is the number of the land-use types.

Table 1. Ecosystem elasticity coefficient of land-use types in the Qinling-Daba Mountains.

LULC type	Resilience	Resistance	EC
Farmland	0.30	0.60	0.51
Forest	0.50	1.00	0.85
Grassland	0.80	0.70	0.73
Impervious surface	0.20	0.30	0.27
Water body	0.70	0.90	0.84
Wetland	0.60	0.80	0.74
Bare land	1.00	0.20	0.44
Glacier and snow	0.10	0.10	0.10

Since each indicator can be quantified by different factors, the value of each indicator needs to be normalized. To avoid magnification when multiplying the indicators during calculation, it is necessary to use a root sign to neutralize the order of magnitude:

$$EH = \sqrt[3]{V \times O \times R} \tag{6}$$

where EH is the regional ecosystem health index of spatial entities, V is the regional ecosystem vigor, O is the regional ecosystem organization, R is the regional ecosystem resilience.

2.3.2. Moran's I Index

Affected by spatial interaction and spatial diffusion, there is a spatial correlation between any entities, but the nearby things are more related to each other [41]. The global Moran's I index is used to measuring the degree of dependence between spatial entities in the whole region, while the local indicator of spatial association (LISA) is used to detect the extent and location of outliers or agglomerations.

$$I = \frac{n}{\sum_{i=1}^{n}\sum_{j=1}^{n} w_{ij}} \times \frac{\sum_{i=1}^{n}\sum_{j=1}^{n} w_{ij}(y_i - \overline{y})(y_j - \overline{y})}{\sum_{i=1}^{n}(y_i - \overline{y})^2} \tag{7}$$

$$I_i = \frac{y_i - \overline{y},}{\frac{1}{n}\sum(y_i - \overline{y})^2} \sum_{j\neq 1}^{n} w_{ij}(y_j - \overline{y}) \tag{8}$$

$$Z = \frac{I - E(I)}{\sqrt{Var(I)}} \tag{9}$$

$$E(I) = \frac{-1}{n-1} \tag{10}$$

$$Var(I) = E\left(I^2\right) - E(I)^2 \tag{11}$$

where I is the global Moran's I value; n is the number of spatial entities; y_i and y_j represent the attribute values of the ith and jth space entities, respectively; $\overline{y}$ is the mean value of all spatial entities attribute values; w_{ij} is weight between spatial entities i and j; I_i represents the LISA value of the ith spatial entity; Z is the threshold for normalized statistics; $E(I)$ is expected autocorrelation; and $Var(I)$ is variance.

2.3.3. Selection of Driving Factors

Ecosystem health is influenced by a combination of natural and anthropogenic factors, and seven drivers were selected based on previous studies [42,43]. Natural factors include annual mean precipitation (AMP), annual mean temperature (AMT), elevation (expressed in DEM), and proportion of forest (PFL), which are related to climate, topography, and vegetation and directly determine the external conditions that affect the ecosystem.

Anthropogenic factors mainly include human-led socioeconomic activities and their altered land use, which indirectly change the corresponding ecological structure and affect ecosystem health. Three main indicators are included: population size (POP), gross regional domestic product (GRDP), and proportion of built-up land (PBL). POP can reflect the intensity of human activities, GRDP can evaluate regional economic development, and PBL can intuitively reflect the expansion of urban space. However, when the seven dependent variables were tested for multicollinearity, it was found that the variance inflation factor (VIF) of AMP and AMT was greater than 10, and there was strong multicollinearity with other variables, so these two variables were excluded. In order to eliminate the influence of units and dimensions, five independent variables were standardized.

2.3.4. Geographically Weighted Regression Model

GWR is widely used in geography and related disciplines involving spatial pattern analysis [44,45] and can be used to quantitatively reflect spatial heterogeneity, as well as to explore geographic variation between response and explanatory variables. The model structure is as follows:

$$\mathrm{y}_i = \beta_0(u_i, v_i) + \sum_{l=1}^{p} \beta_l(u_i, v_i)x_{il} + \varepsilon_i \tag{12}$$

where yi is the fitted value of the ecosystem health for spatial entity i, $\beta_0(u_i, v_i)$ is the coordinates of spatial entity i, $\beta_l(u_i, v_i)x_{il}$ is the lth regression parameter of spatial entity i, ε_i is the error correction term, and p is the number of explanatory variables.

$$\hat{\beta}_k(u_i, v_i) = \left[X^T W(u_i, v_i) X\right]^{-1} X^T W(u_i, v_i) Y \tag{13}$$

where $W(u_i, v_i)$ is an n × n matrix whose diagonal Wij denotes the weight of the influence weight of the jth entity on the ith entity, while the non-diagonal elements are all 0. Wij is generally obtained through the kernel function based on the distance, and the Gaussian kernel function is used in this study. The dependent variable in this study is ecosystem health index, and the independent variable is the corresponding natural and anthropogenic factors. R square (R2), adjusted R2, and Akaike information criterion (AICc) are used to measure the performance of the model. In general, the higher the R2 and adjusted R2 values, and the lower the AICc values, the better the performance of the model.

3. Results

3.1. Spatiotemporal Differentiation of Land Use/Land Cover in the Qinling-Daba Mountains

Significant land-use changes have taken place in the study area (Figure A1). In the Qinling-Daba Mountains, the forest is dominant, accounting for more than 60% of the total area. Forest has increased by 1.9553% (6024 km^2) since 2000 (Table 2), which is the land-use type with the most growth. The impervious surface has also increased significantly, an increase of 1.0566%, which is mainly due to the conversion of farmland to impervious surface. The water area of Danjiangkou has significantly expanded, which is the main source of the increase in the proportion of water body. The grassland area shrank the most, with a decrease of 2.8928% (8913 km^2), especially in the research area in Gansu Province, which was mainly converted into farmland and forest. In 2000 (Figure A1a), 28.6544% (7266 km^2) of the total area was used for agricultural activities, which dropped to approximately 28% in 2020 (Figure A1c), mainly due to the occupation of agricultural land by construction land. However, only slight changes have taken place in wetlands, glacier and snow, and bare land.

Table 2. Percentage of LULC changes in the Qinling-Daba Mountains in 2000, 2010, and 2020 (Unit: km^2).

LULC	2000	2010	2020	Percentage Change
Farmland	28.6544	28.5291	28.0391	−0.6153
Forest	62.3893	64.7448	64.3446	1.9553
Grassland	7.2783	4.5099	4.3855	−2.8928
Wetland	0.0677	0.0764	0.0945	0.0268
Water body	0.6182	0.7990	1.0791	0.4609
Impervious surface	0.9920	1.3407	2.0486	1.0566
Glacier and snow	0.0001	0.0001	0.0003	0.0002
Bare land	0	0	0.0083	0.0083

3.2. Spatiotemporal Changes in Ecosystem Health in the Qinling-Daba Mountains

In this study, the five levels of weak, slightly weak, ordinary, slightly well, and well were classified in equal intervals according to the ascending order of the values. The most pronounced changes were in ecosystem vigor levels and the changes in the level of ecological resilience were the least (Figure 3).

There was an overall upward trend in ecosystem vigor. In 2000, approximately 70% (83) of the counties did not reach a relatively well level, while only one county (Langzhong) was at a relatively weak level in 2020. Among them, Weiyuan and Xichuan crossed two levels from weak to ordinary ecological vigor level in 2020. Compared with ecosystem vigor and ecosystem resilience, the overall level of ecosystem organization in the Qinling-Daba Mountains is slightly lower. The part with weak ecological organization is mainly concentrated within the central Shaanxi and Hubei provinces, with significant regional differences. From 2000 to 2020, the ecological resilience has changed slightly, and more than 70% of the districts and counties have reached a slightly better or above level, but the ecological resilience of Yexian, Wolong, Fancheng, and Xiangzhou has decreased from weak to weak. The change in ecosystem resilience is relatively insignificant. Over 70% of the counties reached slightly well and above levels, but Yexian, Wolong, Fancheng, and Xiangzhou showed a decrease in ecosystem resilience, changing from slightly weak to weak.

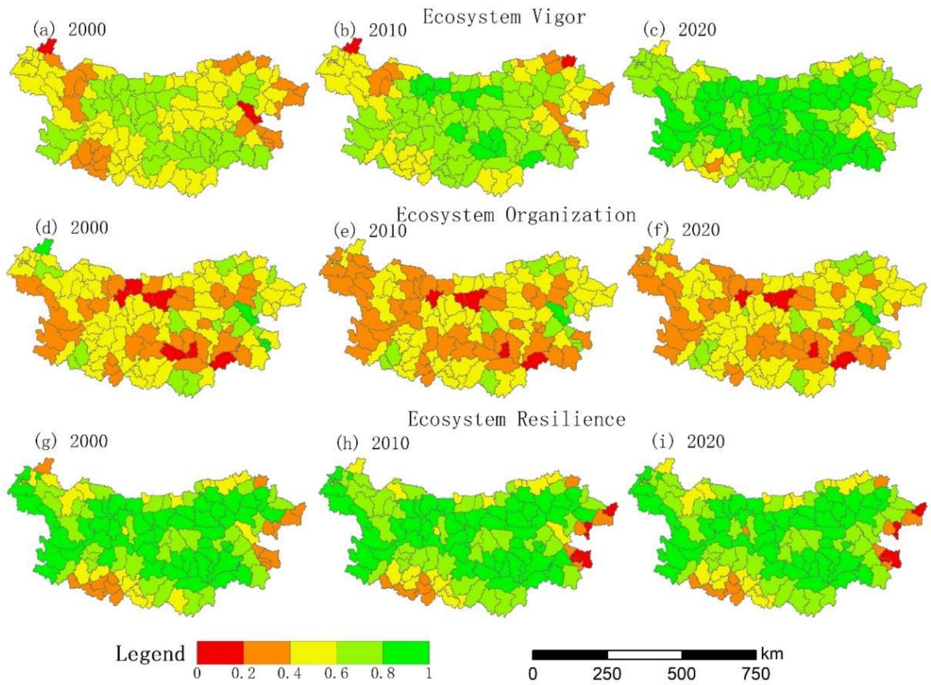

Figure 3. Changes in ecosystem indicators for each county in the Qinling-Daba Mountains from 2000 to 2020. (**a**–**c**) Ecosystem vigor for each county (**d**–**f**) Ecosystem organization for each county (**g**–**i**) Ecosystem resilience for each county.

The changes in ecosystem health in the central and western parts of the study area are significantly greater than in the eastern parts, and the ecosystems in the central and western parts are healthier (Figure 4). From 2000 to 2020, the overall ecosystem health of the research area has improved year by year, and by 2020, 62% (72) of counties had EH values greater than 0.6. The value of ecosystem health in Fancheng and Wolong in the eastern part of the study area showed a significant decline, with Wolong having the lowest level (0.27) among all counties in 2020 (Figure 4c). The ecosystem health value of Xichuan has increased the most, with an increase of 0.18 over 20 years. In 2020, ecosystems in Shiquan, Lushi, Yunyang_HB, and Hanbin are relatively healthier, all reaching 0.7. The ecosystem health at the county level shows a spatial pattern of patchy distribution. The counties with values of 0.5–0.6 in 2000 (Figure 4a) and 2010 (Figure 4b) and 0.6–0.7 in 2010 and 2020 show a clear spatial dependence.

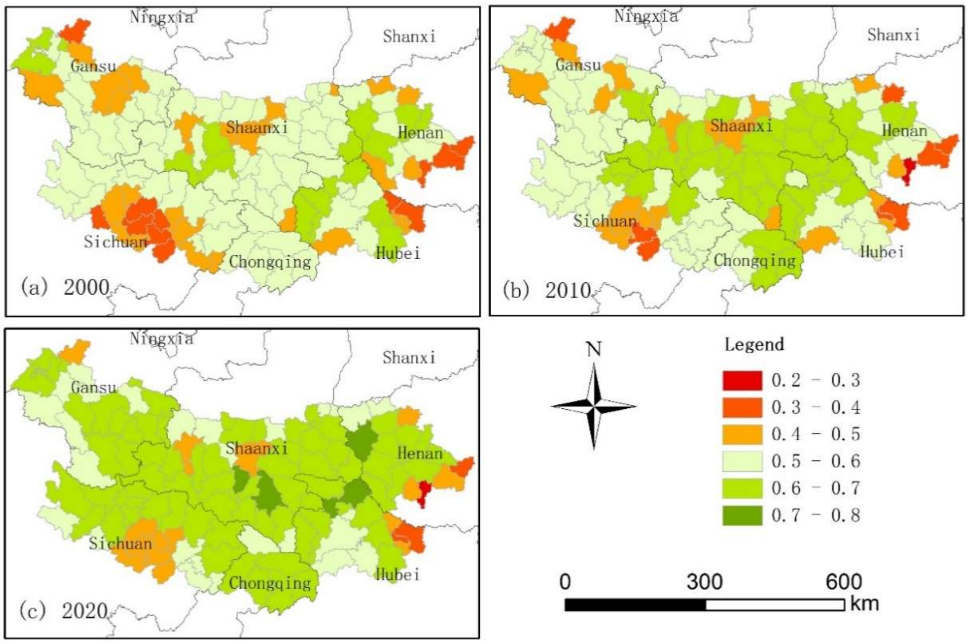

Figure 4. Spatial distribution of comprehensive ecosystem health index at the county level in the Qinling-Daba Mountains from 2000 to 2020.

3.3. Spatial Dependency of Ecosystem Health

This study uses the global Moran's I index to quantitatively measure the spatial autocorrelation of ecosystem health in the entire region. Using GeoDa software, weights based on Rook contiguity were obtained, and the results of 999 random inspections are shown in Appendix B. Rook contiguity refers to when only the common edges of polygons are considered to define the adjacency relationship (common vertices are ignored). The global Moran's I values for 2000, 2010, and 2020 all ranged from 0.38 to 0.42 (Table A1), which were positive and passed the significance test at the 1% level. This indicates that the ecosystem health level of the Qinling-Daba Mountains has significant spatial autocorrelation throughout the region, that is, the level of ecosystem health in each county is more positively influenced by the neighboring counties. In terms of temporal dynamics, the global Moran's I index showed an inverted V-shaped increase. The value increased from 2000 to 2010, indicating that the spatial dependence of ecosystem health has increased, and the ecological pattern tends to be aggregated. From 2010 to 2020, the value slightly decreased, implying that the spatial aggregation of ecosystem health in the study area weakened and the ecological layout showed a trend of diffusion, reflecting the efficacy of promoting the regional synergistic development strategy.

To further explore the local spatial autocorrelation, this paper uses the local indicators of spatial association (LISA) to analyze the spatial aggregation that exists in counties (Figure 5). The High–High type is the main agglomeration type within the Qinling-Daba Mountains and is mainly distributed in the eastern part, indicating that the eastern part gathers counties with high levels of ecosystem health. The High–High type counties in 2000 (Figure 5a) and 2020 (Figure 5c) were distributed in a block-like pattern near the Qinling Mountains, while in 2010 (Figure 5b) they showed a strip-like distribution along the Qinling Mountains, indicating the increased radiation capacity of the eastern region during this period. The Low–Low type counties are mainly distributed in the southwestern and eastern edges of the study area, with small spatial extent variation, indicating that the improvement of counties with poor health is not significant. Low–High and High–Low type counties are extremely rare in the study area, existing between the High–High and Low–Low catchment areas.

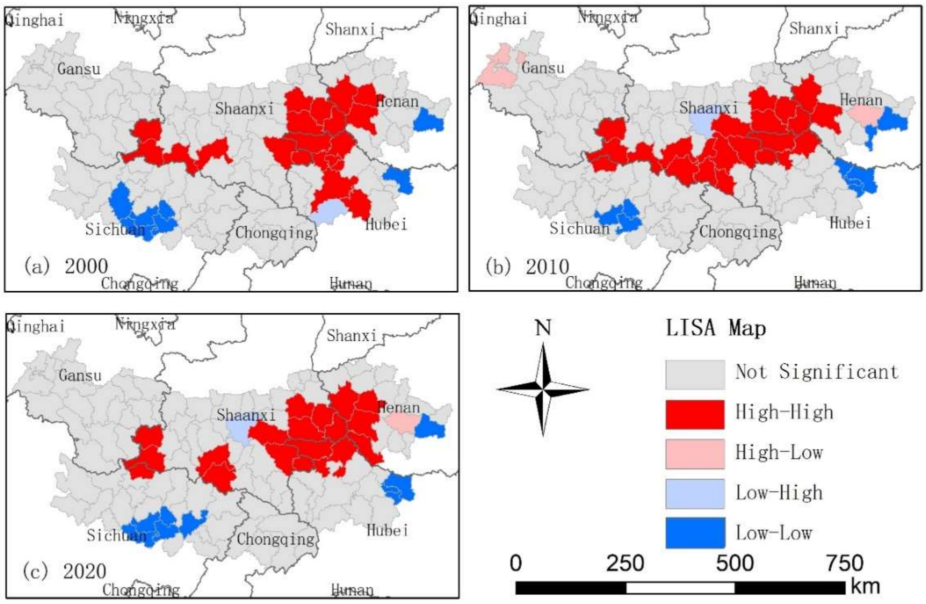

Figure 5. The spatial agglomeration of ecosystem health based on Rook contiguity from 2000 to 2020.

3.4. Analysis of Driving Factors for Ecosystem Health

GWR not only reveals the effects of the five explanatory variables on ecosystem health but also exhibits significant spatial heterogeneity (Figure 6). The regression coefficients of the five explanatory variables for each county were obtained through GWR, and the results showed that the five explanatory variables had both positive and negative effects on ecosystem health. GRDP had a significant inhibitory effect on the eastern part of the Qinling-Daba Mountains, shifting from negative in the northeast to positive in the southwest. In 2000, the impact of GRDP on ecosystem health dominated, especially in Shaanxi and Hubei provinces in the east-central region. However, the negative impact of GRDP diminished over time, and by 2020, the positive and negative effects were similar in the study area. The positive impact of POP appears to decrease from the east to the two sides, and the southwest and northeast of research area have negative effects. It is noteworthy that the positive impact of the central region keeps spreading to the northwest. The negative effect of PBL on EH gradually spreads to the southwest, with a positive effect on only five counties by 2020. The growth of anthropogenic factors (GRDP and PBL) suggests that urbanization is accelerating, but for them, both have varying degrees of inhibition on ecosystem health.

From 2000 to 2020, PFL promoted ecosystem health in the majority of the Qinling-Daba Mountains, while DEM had an inhibitory effect on a wide range of research areas. The positive effect of PFL gradually decreases from southwest to northeast, with a negative effect especially in some counties within Shaanxi Province. The high values of PFL coefficients spread to the northeast, indicating that PFL has an increasingly strong promoting effect on EH. At the same time, the negative effect of PFL on some central regions is also increasing. The high value of the PFL coefficient spread to the northeast, indicating that PFL has become more and more effective in promoting ecosystem health. At the same time, the negative effect of PFL on central regions is also increasing. The positive effect of DEM on ecosystem health is mainly concentrated in the northwest and northeast of the study area and has a negative impact on the rest of the area. The inhibitory effect of DEM on the study area is increasing with time, especially for the southeastern part.

Overall, anthropogenic factors (GRDP and PBL) and the natural factor (DEM) had a strong negative impact on ecosystem health in the Qinling-Daba Mountains, while the natural factor (PFL) had a more positive effect.

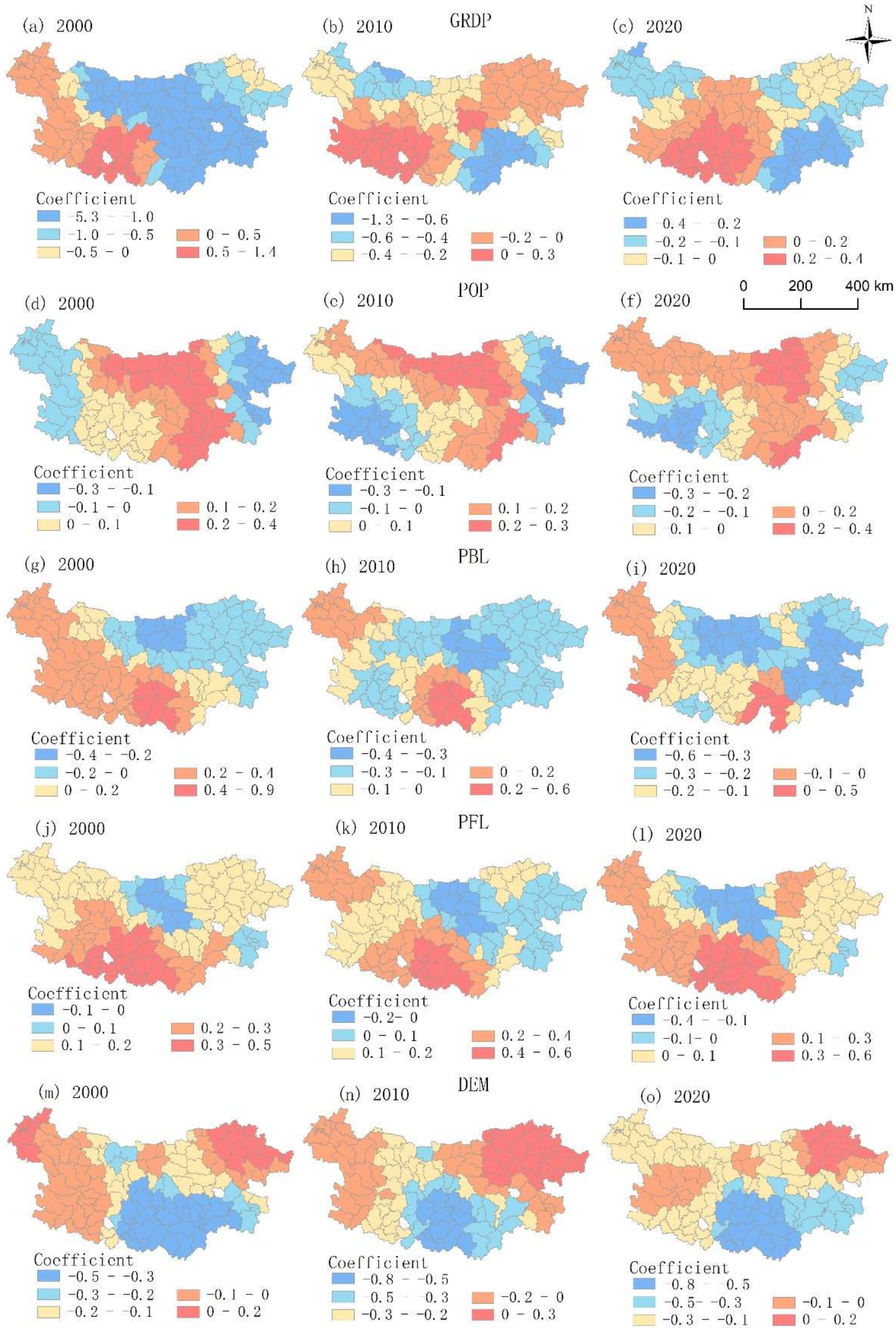

Figure 6. Spatial distribution patterns of correlation coefficients between ecosystem health and driving factors from 2000 to 2020. (**a**–**c**) GRDP: Gross regional domestic product. (**d**–**f**) POP: Population size. (**g**–**i**) PBL: Proportion of built-up land. (**j**–**l**) PFL: Proportion of forest land. (**m**–**o**) DEM: Digital elevation model, reflecting elevation.

4. Discussion

4.1. Methodological Advantages of GWR

Goodness of fit tests for comparing the ordinary least square (OLS) model and GWR model are evaluated by using AICc, R2, and adjusted R2 (Table 3). Compared with the results of the OLS model, the R2 and adjusted R2 of the GWR model are larger than those of the OLS model in 2000, 2010, and 2020, indicating that the GWR better explains the spatial relationship between factors and ecosystem health. Moreover, the GWR model has a smaller AICc than the OLS model, which indicates that the GWR model is better than the OLS model. The adjusted R2 values were all above 0.58%, and the R2 values increased as the years went by, indicating that the GWR model could be used to analyze the effects of each variable on ecosystem health.

Table 3. Statistical results of GWR and OLS in 2000, 2010, and 2020 in the Qinling-Daba Mountains.

	R^2		Adjusted R^2		AICc	
	OLS	**GWR**	**OLS**	**GWR**	**OLS**	**GWR**
2000	0.3883	0.6901	0.3549	0.5802	−310.9931	−340.4735
2010	0.4742	0.7524	0.4455	0.6593	−302.9470	−337.7385
2020	0.4089	0.7830	0.3766	0.6951	−288.1240	−346.3527

The spatial variation of the local R2 of the GWR model from 2000 to 2020, reflecting the spatial variation of the county-level fit (Figure A2). Provinces such as Henan, Hubei, and Sichuan located in the east and southwest have a higher local R2, reaching above 0.7, indicating that the local linear regression model performs well in this region. However, in Gansu and Shaanxi, which are located in the north, the local R2 is relatively low. Especially in 2000 (Figure A2a), there were 32 counties with a local R2 of less than 0.5, while Gansu and Shaanxi provinces occupied 31 counties. In general, the local R2 of the GWR model has improved, and the overall fitting effect tends to be good, which can explain the spatial correlation between ecological health and GRDP, POP, PFL, PBL, and DEM.

4.2. Comparison with Previous Studies

The trends in ecosystem health are the result of a combination of natural and anthropogenic factors, and different drivers play different roles at different times of ecosystem evolution [46]. Anthropogenic factors are more active and dramatic at specific temporal and spatial scales, especially with the increasing level of urbanization [47].

In terms of anthropogenic factors, the transformation of urban land is the main driver of ecosystem health deterioration, which works in conjunction with rapid urbanization to cause the degradation of ecosystem health [14]. However, this study shows that the drivers are not absolutely positive or negative influences, and they have significant regional differences. For example, the negative effect of PBL gradually increases and expands westward, and eventually, its positive effect only exists in the five southern counties. Built-up land is most affected by anthropogenic activities, and the expansion of built-up land leads to a reduction in ecosystem services and ultimately damages ecosystem health [48]. Similar studies have shown that the expansion of urban space can lead to the degradation of ecosystem health [49,50]. GRDP has a dual perturbative effect on ecosystems, manifested as a positive contribution through the implementation of ecological conservation projects and a negative inhibition by rapid urbanization [51]. In the western and eastern parts of the study area, close to urban areas, POP has a negative effect on ecosystem health, which is due to the concentration of population in areas close to cities and more interference from human activities in areas close to cities. In contrast, the central part of the study area is far away from the city, and appropriate human activities are beneficial to ecosystem health.

In terms of natural factors, topography is the basic physical element that affects human life patterns and landscape patterns [50]. Ecosystems at different altitudes have different ecosystem structures [52]. In the Qinling-Daba Mountains, altitude has a negative effect on ecosystem health in most areas. In mountainous ecosystems, where human activities are relatively low and vegetation cover is extensive, ecosystem health degradation is relatively low [53]. Although woodlands are less disturbed by humans, it cannot be ignored that the reduction of vegetation cover also has a negative impact on ecosystem health. The significant and positive effect of PFL on ecosystem health is apparent in most areas, but its negative impact is gradually deepening and spreading. The high vegetation cover in mountainous ecosystems and its effect on ecosystem improvement decreases when vegetation cover reaches a certain level [54]. Similar studies have also found that meteorological factors such as AMP and AMT have significant effects on ecosystem health in regional ecosystem evolution [55,56]. However, meteorological factors were not considered in this study because they failed the multiple covariance tests and were, therefore, not considered as influencing factors, probably due to differences in study areas and time periods.

4.3. Policy Implications

The analysis of county-level ecosystem health and its drivers contribute to the development of ecological health at small scales from a scientific perspective and provide a scientific basis for policymakers to develop relevant policies [57,58]. Based on the findings, we identified regional differences in ecosystem health and its key drivers, so ecological conservation measures taken in a specific area should be adjusted according to the ecosystem health level and its drivers. (1) For some regions on the eastern and southwestern fringes, the level of ecological health is poor, and anthropogenic factors have a negative impact. The level of spatial expansion in these areas exceeds the local ecological carrying level, and the population should be appropriately evacuated, the amount of construction land exploitation should be reduced, green industries should be encouraged, and the ecological environment should be restored. (2) For areas at moderate ecosystem health levels, mainly attributed to low ecosystem organization and human factors (GRDP, PBL), sustainable development needs to be maintained to balance economic growth and ecological conservation. For example, in some marginal counties in the northwest and southeast, it is necessary to optimize the land-use structure and avoid unreasonable reclamation and construction to increase ecosystem organization. At the same time, it is necessary to control the scale of urban and rural areas, implement more ecological protection and restoration projects, focus on the layout of green low-impact industries, and carry out green industrial development within the environmental carrying capacity. (3) For most areas with a high level of ecosystem health in the western and central regions, high forest coverage has a promoting effect. These counties have high ecological value and high ecological sensitivity and need to implement strict ecological protection.

The empirical results of our study suggest that ecosystem health is influenced by both natural and anthropogenic factors, as well as by spatial context. Ecosystem health in a county is influenced not only by elements in that county but also by elements in neighboring counties [59]. Areas with healthy ecosystems may promote the improvement of areas with deteriorating ecosystems, and conversely, areas with deteriorating ecosystems may delay the optimization of areas with healthy ecosystems, leading to a significant spatial correlation in ecosystem health. Therefore, the formulation and implementation of policies on regional economic layout and territorial spatial planning cannot be limited to individual administrative units [60] but require a deeper understanding of the spatial interactions of ecosystems.

4.4. Limitations and Future Work

The study area is dominated by mountainous hills, which can be representative of mountainous areas in China, but there is an insufficient explanation for other topographical features. The ecosystem is a complex system. Ecosystem vigor, ecosystem organization, and ecosystem resilience are its three very important aspects, but there are still some other aspects that deserve attention, such as ecosystem services, ecosystem values, etc. Compared to others' studies, this study analyzed the influencing factors of ecosystem health, but the selection of anthropogenic factors was somewhat limited due to the different statistical indicators in each county. In the future, a detailed analysis of soils and climates could help to elucidate the deep mechanisms of change in ecosystem health and the joint effects of changes.

Despite the limitations, we still believe this study is meaningful. While the number of metrics is somewhat small, the quantification of data processing is by no means arbitrary. Geographically weighted regression models can not only study the importance of drivers and their interactions on ecosystem health but also visualize spatial heterogeneity in the form of maps. The results can help researchers understand the spatial pattern of changes in ecosystem health and provide a scientific basis for ecological protection and make comments and suggestions to the relevant government agencies.

5. Conclusions

In this paper, we analyzed the dynamics of the ecosystem health of 120 districts and counties within the Qinling-Daba Mountains in 2000, 2010, and 2020 and analyzed the driving factors in different regions using the GWR model. From the results, we obtained the following conclusions.

(1) Land-use changes are obvious in the Qinling-Daba Mountains, with the largest increases in forest and impervious surface and large decreases in agricultural land and grassland. This result indicates that afforestation efforts in the study area were effective, and the expansion of forest and urban space has taken up a large amount of farmland and grassland.
(2) The overall ecological health of the Qinling-Daba Mountains is on the rise, with the best ecosystem health status emerging in Shiquan, Lushi, Yunyang_HB, and Hanbin. However, ecosystem health deteriorated in some areas, with Fancheng and Wolong being the most obvious.
(3) There is a clear spatial correlation in ecosystem health. The High–High type counties with healthy ecosystems are mainly concentrated near the Qinling Mountains, indicating the overall high level of ecological health in this region.
(4) Anthropogenic and natural factors have a bidirectional effect on ecosystem health in the Qinling-Daba Mountains. The positive effect of GRDP gradually shifts to the central region, while the negative effect of PBL spreads to the west, indicating that the urban space in the western region is expanding. PFL has a catalytic effect on the ecosystem health in most areas, so afforestation is an effective measure to protect the ecology.

Research on ecosystem health can help protect the ecological environment, and identifying the contribution of different factors can help decision-makers to make better develop management plans and promote the coordination between regional development and ecological protection.

Author Contributions: Ting Xiang: conceptualization, methodology, software, writing—original draft and revision. Xiaoliang Meng: writing—reviewing and editing. Xinshuang Wang: resources, data curation. Jing Xiong: resources, data curation. Zelin Xu: conceptualization, formal analysis. All authors have read and agreed to the published version of the manuscript.

Funding: This research was funded by National Natural Science Foundation of China (NSFC) under grant number 41971352. The authors are very grateful to the many people who helped to comment on the article, and the Large Scale Environment Remote Sensing Platform (Facility No. 16000009, 16000011, 16000012) provided by Wuhan University.

Data Availability Statement: Not applicable.

Acknowledgments: Special thanks to the editors and reviewers for providing valuable insight into this article.

Conflicts of Interest: The authors declare no conflict of interest.

Appendix A

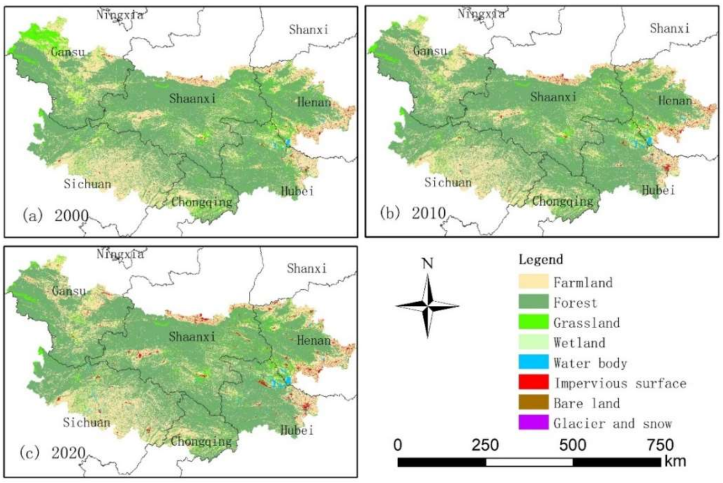

Figure A1. Land-use patterns in the Qinling-Daba Mountains in 2000, 2010, and 2020.

Appendix B

Table A1. Global Moran's I statistics of ecosystem health.

Year	Moran's I	Z	P
2000	0.3787	7.0974	0.001
2010	0.4119	7.5573	0.001
2020	0.4007	7.4086	0.001

Appendix C

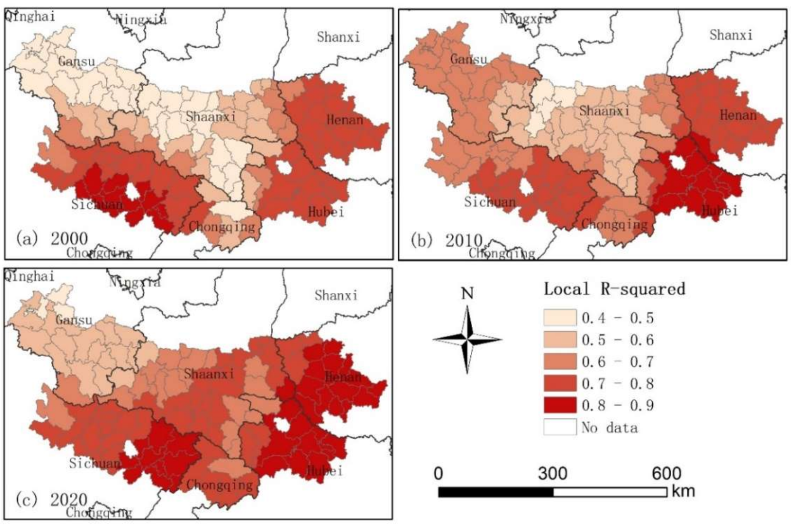

Figure A2. Spatial mapping of the locally weighted coefficient of determination (R2) between the observed and fitted values is performed by GWR modeling at the county level.

References

1. Huang, Z.; Du, X.; Castillo, C.S.Z. How does urbanization affect farmland protection? Evidence from China. *Resour. Conserv. Recycl.* **2019**, *145*, 139–147. [CrossRef]
2. Dadashpoor, H.; Azizi, P.; Moghadasi, M. Land use change, urbanization, and change in landscape pattern in a metropolitan area. *Sci. Total Environ.* **2019**, *655*, 707–719. [CrossRef] [PubMed]
3. Franco, S.; Mandla, V.R.; Rao, K.R.M. Urbanization, energy consumption and emissions in the Indian context A review. *Renew. Sustain. Energy Rev.* **2017**, *71*, 898–907. [CrossRef]
4. Wang, S.; Gao, S.; Li, S.; Feng, K. Strategizing the relation between urbanization and air pollution: Empirical evidence from global countries. *J. Clean. Prod.* **2020**, *243*, 118615. [CrossRef]
5. Sanderson, E.W.; Walston, J.; Robinson, J.G. From bottleneck to breakthrough: Urbanization and the future of biodiversity conservation. *BioScience.* **2018**, *68*, 412. [CrossRef]
6. Su, M.; Fath, B.D.; Yang, Z. Urban ecosystem health assessment: A review. *Sci. Total Environ.* **2010**, *408*, 2425–2434. [CrossRef] [PubMed]
7. Rapport, D.J.; Maffi, L. Eco-cultural health, global health, and sustainability. *Ecol. Res.* **2011**, *26*, 1039–1049. [CrossRef]
8. Douglas, I. Urban ecology and urban ecosystems: Understanding the links to human health and well-being. *Curr. Opin. Environ. Sustain.* **2012**, *4*, 385–392. [CrossRef]
9. Yu, G.; Yu, Q.; Hu, L.; Zhang, S.; Fu, T.; Zhou, X.; He, X.; Liu, Y.; Wang, S.; Jia, H. Ecosystem health assessment based on analysis of a land use database. *Appl. Geogr.* **2013**, *44*, 154–164. [CrossRef]
10. Liu, D.; Hao, S. Ecosystem health assessment at county-scale using the pressure-state-response framework on the Loess Plateau, China. *Int. J. Environ. Res. Public Health* **2017**, *14*, 2. [CrossRef]
11. Sun, B.; Tang, J.; Yu, D.; Song, Z.; Wang, P. Ecosystem health assessment: A PSR analysis combining AHP and FCE methods for Jiaozhou Bay, China1. *Ocean Coast Manage* **2019**, *168*, 41–50. [CrossRef]
12. Jafary, P.; Sarab, A.A.; Tehrani, N.A. Ecosystem health assessment using a fuzzy spatial decision support system in Taleghan watershed before and after dam construction. *Environ. Process.* **2018**, *5*, 807–831. [CrossRef]
13. Malekmohammadi, B.; Jahanishakib, F. Vulnerability assessment of wetland landscape ecosystem services using driver-pressure-state-impact-response (DPSIR) model. *Ecol. Indic.* **2017**, *82*, 293–303. [CrossRef]
14. Peng, J.; Liu, Y.; Wu, J.; Lv, H.; Hu, X. Linking ecosystem services and landscape patterns to assess urban ecosystem health: A case study in Shenzhen City, China. *Landscape Urban Plan.* **2015**, *143*, 56–68. [CrossRef]
15. Xiao, R.; Liu, Y.; Fei, X.; Yu, W.; Zhang, Z.; Meng, Q. Ecosystem health assessment: A comprehensive and detailed analysis of the case study in coastal metropolitan region, eastern China. *Ecol. Indic.* **2019**, *98*, 363–376. [CrossRef]
16. Das, M.; Das, A.; Mandal, A. Research note: Ecosystem Health (EH) assessment of a rapidly urbanizing metropolitan city region of eastern India–A study on Kolkata Metropolitan Area. *Landsc. Urban Plan.* **2020**, *204*, 103938. [CrossRef]
17. Bae, D.Y.; Kumar, H.K.; Han, J.H.; Kim, J.Y.; Kim, K.W.; Kwon, Y.H.; An, K.G. Integrative ecological health assessments of an acid mine stream and in situ pilot tests for wastewater treatments. *Ecol. Eng.* **2010**, *36*, 653–663. [CrossRef]
18. Bebianno, M.J.; Pereira, C.G.; Rey, F.; Cravo, A.; Duarte, D.; d'Errico, G.; Regoli, F. Integrated approach to assess ecosystem health in harbor areas. *Sci. Total Environ.* **2015**, *514*, 92–107. [CrossRef]
19. Cheng, X.; Chen, L.; Sun, R.; Kong, P. Land use changes and socio-economic development strongly deteriorate river ecosystem health in one of the largest basins in China. *Sci. Total Environ.* **2018**, *616*, 376–385. [CrossRef]
20. He, J.; Pan, Z.; Liu, D.; Guo, X. Exploring the regional differences of ecosystem health and its driving factors in China. *Sci. Total Environ.* **2019**, *673*, 553–564. [CrossRef]
21. Xie, G.; Zhang, C.; Zhen, L.; Zhang, L. Dynamic changes in the value of China's ecosystem services. *Ecosyst. Serv.* **2017**, *26*, 146–154. [CrossRef]
22. Wang, S.; Fang, C.; Ma, H.; Wang, Y.; Qin, J. Spatial differences and multi-mechanism of carbon footprint based on GWR model in provincial China. *J. Geogr. Sci.* **2014**, *24*, 612–630. [CrossRef]
23. Zhu, C.; Zhang, X.; Zhou, M.; He, S.; Gan, M.; Yang, L.; Wang, K. Impacts of urbanization and landscape pattern on habitat quality using OLS and GWR models in Hangzhou, China. *Ecol. Indic.* **2020**, *117*, 106654. [CrossRef]
24. Zhang, H.; Gao, Y.; Hua, Y.; Zhang, Y.; Liu, K. Assessing and mapping recreationists' perceived social values for ecosystem services in the Qinling Mountains, China. *Ecosyst. Serv.* **2019**, *39*, 101006. [CrossRef]
25. Fan, J.; Li, J.; Xia, R.; Hu, L.; Wu, X.; Li, G. Assessing the impact of climate change on the habitat distribution of the giant panda in the Qinling Mountains of China. *Ecol. Model.* **2014**, *274*, 12–20. [CrossRef]
26. Lu, C.Y.; Gu, W.; Dai, A.H.; Wei, H.Y. Assessing habitat suitability based on geographic information system (GIS) and fuzzy: A case study of Schisandra sphenanthera Rehd. et Wils. in Qinling Mountains, China. *Ecol. Model.* **2012**, *242*, 105–115. [CrossRef]
27. Liu, X.; Zhu, X.; Pan, Y.; Li, S.; Ma, Y.; Nie, J. Vegetation dynamics in Qinling-Daba Mountains in relation to climate factors between 2000 and 2014. *J. Geogr. Sci.* **2016**, *26*, 45–58. [CrossRef]
28. Bai, Y. Analysis of vegetation dynamics in the Qinling-Daba Mountains region from MODIS time series data. *Ecol. Indic.* **2021**, *129*, 108029. [CrossRef]
29. Dang, H.; Zhang, Y.; Zhang, K.; Jiang, M.; Zhang, Q. Age structure and regeneration of subalpine fir (Abies fargesii) forests across an altitudinal range in the Qinling Mountains, China. *For. Ecol. Manag.* **2010**, *259*, 547–554. [CrossRef]

30. Shao, Y.; Mu, X.; He, Y.; Sun, W.; Zhao, G.; Gao, P. Spatiotemporal variations of extreme precipitation events at multi-time scales in the Qinling-Daba mountains region, China. *Quatern Int.* **2019**, *525*, 89–102. [CrossRef]
31. Hu, Y.; Yao, Y.; Kou, Z. Exploring on the climate regionalization of Qinling-Daba mountains based on Geodetector-SVM model. *PLoS ONE* **2020**, *15*, e0241047. [CrossRef]
32. Yu, Y.; Li, J.; Zhou, Z.; Ma, X.; Zhang, X. Response of multiple mountain ecosystem services on environmental gradients: How to respond, and where should be priority conservation? *J. Clean. Prod.* **2021**, *278*, 123264. [CrossRef]
33. Li, J.; Zhang, L.; Ye, H. Spatiotemporal Change Analysis of Annual Average NDVI in Qinling Mountains as Ecological Security Barrier and Dividing Line between Geography and Climate. *IOP Conf. Ser. Earth Environ. Sci.* **2021**, *804*, 022108. [CrossRef]
34. Costanza, R. Toward an operational definition of ecosystem health. In Ecosystem Health: New Goals for Environmental Management. In *Frontiers in Ecological Economics*; Edward Elgar Publishing: Cheltenham, UK, 1997; pp. 239–269.
35. Nemani, R.R.; Keeling, C.D.; Hashimoto, H.; Jolly, W.M.; Piper, S.C.; Tucker, C.J.; Myneni, R.B.; Running, S.W. Climate-driven increases in global terrestrial net primary production from 1982 to 1999. *Science* **2003**, *300*, 1560–1563. [CrossRef]
36. Li, Y.; Cao, Z.; Long, H.; Liu, Y.; Li, W. Dynamic analysis of ecological environment combined with land cover and NDVI changes and implications for sustainable urban–rural development: The case of Mu Us Sandy Land, China. *J. Clean. Prod.* **2017**, *142*, 697–715. [CrossRef]
37. Carlson, T.N.; Ripley, D.A. On the relation between NDVI, fractional vegetation cover, and leaf area index. *Remote Sens Environ.* **1997**, *62*, 241–252. [CrossRef]
38. Pettorelli, N.; Vik, J.O.; Mysterud, A.; Gaillard, J.M.; Tucker, C.J.; Stenseth, N.C. Using the satellite-derived NDVI to assess ecological responses to environmental change. *Trends Ecol. Evol.* **2005**, *20*, 503–510. [CrossRef] [PubMed]
39. Jiang, Z.; Huete, A.R.; Chen, J.; Chen, Y.; Li, J.; Yan, G.; Zhang, X. Analysis of NDVI and scaled difference vegetation index retrievals of vegetation fraction. *Remote Sens Environ.* **2006**, *101*, 366–378. [CrossRef]
40. Peng, J.; Liu, Y.; Li, T.; Wu, J. Regional ecosystem health response to rural land use change: A case study in Lijiang City, China. *Ecol. Indic.* **2017**, *72*, 399–410. [CrossRef]
41. Tobler, W.R. A computer movie simulating urban growth in the Detroit region. *Econ. Geogr.* **1970**, *46* (Suppl. S1), 234–240. [CrossRef]
42. Fang, L.; Wang, L.; Chen, W.; Sun, J.; Cao, Q.; Wang, S.; Wang, L. Identifying the impacts of natural and human factors on ecosystem service in the Yangtze and Yellow River Basins. *J. Clean. Prod.* **2021**, *314*, 127995. [CrossRef]
43. Chen, S.; Feng, Y.; Tong, X.; Liu, S.; Xie, H.; Gao, C.; Lei, Z. Modeling ESV losses caused by urban expansion using cellular automata and geographically weighted regression. *Sci. Total Environ.* **2020**, *712*, 136509. [CrossRef] [PubMed]
44. Yu, H.; Gong, H.; Chen, B.; Liu, K.; Gao, M. Analysis of the influence of groundwater on land subsidence in Beijing based on the geographical weighted regression (GWR) model. *Sci. Total Environ.* **2020**, *738*, 139405. [CrossRef] [PubMed]
45. Wang, Q.; Feng, H.; Feng, H.; Yu, Y.; Li, J.; Ning, E. The impacts of road traffic on urban air quality in Jinan based GWR and remote sensing. *Sci. Rep.* **2021**, *11*, 15512. [CrossRef]
46. Wu, X.; Liu, S.; Zhao, S.; Hou, X.; Xu, J.; Dong, S.; Liu, G. Quantification and driving force analysis of ecosystem services supply, demand and balance in China. *Sci. Total Environ.* **2019**, *652*, 1375–1386. [CrossRef] [PubMed]
47. Zhang, D.; Huang, Q.; He, C.; Wu, J. Impacts of urban expansion on ecosystem services in the Beijing-Tianjin-Hebei urban agglomeration, China: A scenario analysis based on the shared socioeconomic pathways. *Resour. Conserv. Recycl.* **2017**, *125*, 115–130. [CrossRef]
48. Zhang, Y.; Yin, H.; Zhu, L.; Miao, C. Landscape Fragmentation in Qinling–Daba Mountains Nature Reserves and Its Influencing Factors. *Land* **2021**, *10*, 1124. [CrossRef]
49. Mitchell, M.G.; Suarez-Castro, A.F.; Martinez-Harms, M.; Maron, M.; McAlpine, C.; Gaston, K.J.; Johansen, K.; Rhodes, J.R. Reframing landscape fragmentation's effects on ecosystem services. *Trends Ecol. Evol.* **2015**, *30*, 190–198. [CrossRef] [PubMed]
50. Chen, W.; Gu, T.; Zeng, J. Urbanisation and ecosystem health in the Middle Reaches of the Yangtze River urban agglomerations, China: A U-curve relationship. *J. Environ. Manag.* **2022**, *318*, 115565. [CrossRef] [PubMed]
51. Zhang, Z.; Gao, J.; Fan, X.; Lan, Y.; Zhao, M. Response of ecosystem services to socioeconomic development in the Yangtze River Basin, China. *Ecol. Indic.* **2017**, *72*, 481–493. [CrossRef]
52. Locatelli, B.; Lavorel, S.; Sloan, S.; Tappeiner, U.; Geneletti, D. Characteristic trajectories of ecosystem services in mountains. *Front. Ecol. Environ.* **2017**, *15*, 150–159. [CrossRef]
53. Yin, L.; Dai, E.; Zheng, D.; Wang, Y.; Ma, L.; Tong, M. What drives the vegetation dynamics in the Hengduan Mountain region, southwest China: Climate change or human activity? *Ecol. Indic.* **2020**, *112*, 106013. [CrossRef]
54. Ma, S.; Wang, L.J.; Jiang, J.; Chu, L.; Zhang, J.C. Threshold effect of ecosystem services in response to climate change and vegetation coverage change in the Qinghai-Tibet Plateau ecological shelter. *J. Clean. Prod.* **2021**, *318*, 128592. [CrossRef]
55. Fu, Q.; Li, B.; Hou, Y.; Bi, X.; Zhang, X. Effects of land use and climate change on ecosystem services in Central Asia's arid regions: A case study in Altay Prefecture, China. *Sci. Total Environ.* **2017**, *607*, 633–646. [CrossRef] [PubMed]
56. Hao, R.; Yu, D.; Liu, Y.; Liu, Y.; Qiao, J.; Wang, X.; Du, J. Impacts of changes in climate and landscape pattern on ecosystem services. *Sci. Total Environ.* **2017**, *579*, 718–728. [CrossRef] [PubMed]
57. Kang, P.; Chen, W.; Hou, Y.; Li, Y. Linking ecosystem services and ecosystem health to ecological risk assessment: A case study of the Beijing-Tianjin-Hebei urban agglomeration. *Sci. Total Environ.* **2018**, *636*, 1442–1454. [CrossRef]

58. Tang, D.; Liu, X.; Zou, X. An improved method for integrated ecosystem health assessments based on the structure and function of coastal ecosystems: A case study of the Jiangsu coastal area, China. *Ecol. Indic.* **2018**, *84*, 82–95. [CrossRef]
59. Chi, G.; Marcouiller, D.W. Natural amenities and their effects on migration along the urban–rural continuum. *Ann. Reg. Sci.* **2013**, *50*, 861–883. [CrossRef]
60. Chi, G.; Ho, H.C. Population stress: A spatiotemporal analysis of population change and land development at the county level in the contiguous United States, 2001–2011. *Land Use Policy* **2018**, *70*, 128–137. [CrossRef]